Separation Science and Technology
Publication details, including instructions for authors and subscription information:
http://www.informaworld.com/smpp/title~content=t713708471

Adsorption of Phenol and Nitrophenol Isomers onto Montmorillonite Modified with Hexadecyltrimethylammonium Cation

Sung C. Kwon; Dong I. Song; Young W. Jeon

To cite this Article Kwon, Sung C. , Song, Dong I. and Jeon, Young W.(1998) 'Adsorption of Phenol and Nitrophenol Isomers onto Montmorillonite Modified with Hexadecyltrimethylammonium Cation', Separation Science and Technology, 33: 13, 1981 — 1998

To link to this Article: DOI: 10.1080/01496399808545041

URL: http://dx.doi.org/10.1080/01496399808545041

SEPARATION SCIENCE AND TECHNOLOGY, 33(13), pp. 1981–1998, 1998

Adsorption of Phenol and Nitrophenol Isomers onto Montmorillonite Modified with Hexadecyltrimethylammonium Cation

SUNG C. KWON and DONG I. SONG
DEPARTMENT OF CHEMICAL ENGINEERING

YOUNG W. JEON*
DEPARTMENT OF ENVIRONMENTAL ENGINEERING

KYUNGPOOK NATIONAL UNIVERSITY
TAEGU 702-701, SOUTH KOREA

ABSTRACT

Single- and two-component competitive adsorptions were carried out in a batch adsorber to investigate the adsorption behavior of phenol and 2-, 3-, and 4-nitrophenols in aqueous solution at 25°C onto hexadecyltrimethylammonium (HDTMA)-treated montmorillonite. HDTMA cation was exchanged for metal cations on the montmorillonite to prepare HDTMA–montmorillonite, changing its surface property from hydrophilic to organophilic. Effective solid diffusivity of HDTMA cation in the montmorillonite particle was estimated to be about 3×10^{-12} cm^2/s by fitting the film-solid diffusion model to a set of HDTMA adsorption kinetic data onto montmorillonite. Adsorption affinity on HDTMA–montmorillonite was found to be in the order 3-nitrophenol ≈ 4-nitrophenol > 2-nitrophenol > phenol. The Langmuir and the Redlich–Peterson (RP) adsorption models were used to analyze the single component adsorption equilibria. The ideal adsorbed solution theory (IAST) and the Langmuir competitive model (LCM) were used to predict the multicomponent competitive adsorption equilibria. These models yielded favorable representations of both individual and competitive adsorption behaviors.

---

* To whom correspondence should be addressed.

www.dekker.com

INTRODUCTION

Removal of organic contaminants from wastewater has been extensively studied by using various physicochemical and biological techniques. Among these techniques, removal of organic contaminants using organically modified clays has drawn much attention. Natural clays, which are inherently hydrophilic, become organophilic by ion-exchanging a quaternary amine cation having short or long hydrocarbon chains for the metal cations on the clay. Pyrophyllite, which is the parent material of montmorillonite, has a 2:1-type layer, consisting of one octahedral sheet of alumina in the center and two tetrahedral sheets of silica above and below the alumina sheet. Montmorillonite is related to pyrophyllite by the isomorphic substitution of approximately one in six of the aluminum ions in the central octahedral sheet by magnesium or other divalent ions. Among the various types of clay minerals, montmorillonite, the main component of bentonite rock (in general up to 80% by weight), is the usual choice for use as a model support medium due to its large internal surface area, interlayer swelling in water, and high cation-exchange capacity (CEC).

Many investigators have studied sorption of organic contaminants in aqueous solution using organo-clays. Mortland et al. (1) and Boyd et al. (2) studied the uptake of phenol and chlorophenols using smectites ion-exchanged with hexadecyltrimethylammonium (HDTMA) cation. Smectites designate the whole group of montmorillonite (i.e., montmorillonoids) which vary in type and degree of isomorphic substitution. Boyd et al. (3) studied the uptake of benzene and trichloroethylene onto HDTMA–smectite. They found that sorption is mainly effected by the partitioning in the organic phase formed by the conglomeration of large C_{16} alkyl chains from HDTMA cation. Kim et al. (4) studied the uptake of phenolic compounds with an electron-withdrawing group, such as 2-chloro-, 3-cyano-, and 4-nitrophenols, from water onto HDTMA–montmorillonite. They found that the adsorption affinity was in the order 2-chlorophenol > 4-nitrophenol > 3-cyanophenol due to both van der Waals interaction between the long chain hydrocarbon of HDTMA cation and a solute and the steric hinderance.

Lee et al. (5) studied the sorption of benzene, toluene, and *o*-xylene on tetramethylammonium (TMA)–smectite. They reported that the uptake of benzene was larger on TMA–smectite than on HDTMA–smectite, despite the fact that TMA–smectite has a much lower organic carbon content (4%) than HDTMA–smectite (17%). They also found that TMA–smectite exhibited a high degree of selectivity based on the size and shape of an adsorbate in the presence of water, as evidenced by a progressive reduction in uptake with the increase in molecular size from benzene to larger aromatic compounds. This unique selectivity in an aqueous system was attributed to molecular size/shape of adsorbates as well as water molecules which may weakly hydrate TMA cations and solvate mineral sites of TMA–smectite, thereby resulting in insufficient interlamellar space to accommodate relatively larger molecules. Cadena (6) studied the adsorption of benzene, toluene, and *o*-xylene on TMA–bentonite in various pH conditions. According to his results, pH did not affect the adsorption of the nonionizing organics on TMA–bentonite, while benzene was selectively sorbed in the interlamellar space.

Recently, Smith and Galan (7) modified bentonite by exchanging two classes of quaternary amine cations, both the short-chain alkyl or aryl functional groups and long-chain alkyl groups (more than 10 carbons), for the metal cations on bentonite in order to take advantage of both the short- and long-chain functional groups of amine cations involved. They studied sorptions of tetrachloromethane, trichloroethene, and benzene to the dual cation bentonite from water. Lee et al. (8) modified montmorillonite with both HDTMA and TMA cations (i.e., a dual 40% TMA/45% HDTMA–montmorillonite), and studied the sorption of 2-chloro-, 3-cyano-, and 4-nitrophenols from water, resulting in the same order of adsorption affinity as onto the HDTMA–montmorillonite, i.e., 2-chlorophenol > 4-nitrophenol > 3-cyanophenol. They reported that HDTMA plays a much larger role in enhancing the adsorption capacity for the phenolic compounds than does TMA, and the adsorption levels are approximately proportional to the total amount of organic carbon loaded on the montmorillonite.

Although these organo-clays find growing use as landfill liners for contaminant containment and retardation and fuel spill control (9), fundamental studies on sorption and competitive adsorption behaviors have not been completed. In this work we analyze the adsorption kinetics of HDTMA cation onto montmorillonite using the solid diffusion model and taking into account the external liquid film mass transfer between the bulk solution and the particle surface. We chose a homologous series of phenols as solutes [phenol, 2-nitrophenol (2-NiP), 3-nitrophenol (3-NiP), and 4-nitrophenol (4-NiP)] to elucidate the effect of the substitution position of the electron-withdrawing nitro group on sorption behavior. Experimental isotherms and analyses that quantify the single component and binary competitive adsorptions of the phenol and three nitrophenol isomers from water onto the HDTMA–montmorillonite are presented below.

EXPERIMENTAL

Materials

Montmorillonite-KSF was purchased from Aldrich Chemical Co., and the impurities contained were removed by a digestion method using H_2O_2 (10). The digested montmorillonite particles were collected by gravity settling after washing with distilled water. According to Kim et al. (4), the average particle

TABLE 1
Physicochemical Properties of Phenolic Compounds Used

	MW	pK_a	Solubility (g/L)	Total surface area[a] (Å^2)	UV wavelength
Phenol	94.11	9.92	8.2 at 15°C	240	270
2-NiP	139.11	7.23	1.1 at 20°C	299	278
3-NiP	139.11	8.23	13 at 25°C	299	274, 330[b]
4-NiP	139.11	7.08	11 at 20°C	299	318

[a] Data from Yen (15), assuming isomers have identical values.
[b] In the case of bisolute systems with phenol or 2-NiP.

diameter of the collected montmorillonite was about 15 μm, and the CEC and BET surface area were 50.4 meq/100 g-clay and 97 m^2/g-clay, respectively. The cation used as an organic modifier, hexadecyltrimethylammonium (HDTMA) chloride (25 wt%) aqueous solution, was obtained from Aldrich Chemical Co. and used as received. The four phenolic compounds used as adsorbates were phenol, 2-nitrophenol (99 + %), 3-nitrophenol (99%), and 4-nitrophenol (99 + %), purchased from Aldrich Chemical Co. All other reagents were of analytical grade and used as received without further purification.

Preparation of HDTMA–Montmorillonite

HDTMA–montmorillonites were prepared following the procedures employed by Kim et al. (4) and were utilized in the subsequent adsorption experiments of the phenolic compounds. According to Kim et al. (4), the maximum uptake of HDTMA was found to be about 152 mg/g clay, which corresponds to approximately 95% of the CEC of the montmorillonite used in this study.

Adsorption of Phenolic Compounds

Adsorption isotherms on HDTMA–montmorillonite were obtained for the aqueous solutions of four phenolic compounds in a batch reactor at 25°C. Table 1 lists the physicochemical properties of the four phenolic compounds used in this work. Throughout the time study of adsorption of each phenolic compound, it was observed that adsorption equilibrium was reached in about 2 hours on an orbit shaker revolving at 250 rpm. To assure equilibrium, the sample batches were agitated for 24 hours.

We prepared 20 mL solutions of each phenolic compound at various concentrations within the solubility limit. Each solution was poured into a capped 50 mL flask containing 0.5 g of HDTMA–montmorillonite, and then vigorously shaken on an orbit shaker for 24 hours at 25°C. The solutions were then centrifuged at 2000 rpm for 20 minutes. The equilibrium concentrations of each solution were determined at the wavelengths of UV maxima using a UV-Visible spectrophotometer (Hewlett-Packard 8452A, USA).

Four bisolute systems of phenol/3-NiP, phenol/4-NiP, 2-NiP/3-NiP, and 3-NiP/4-NiP were prepared by mixing two phenolic compounds in a 1 : 1 ratio into a 20-mL solution. For the 3-NiP/4-NiP system where the two components show a similar adsorptive affinity for HDTMA–montmorillonite, the two phenolic compounds were also mixed in a 2 : 1 ratio to form a 20-mL solution. We performed bisolute adsorption experiments for the various initial concentrations with a fixed amount (0.5 g) of HDTMA–montmorillonite, following the same procedures as described for the single solute adsorption experiment. In addition, for the 3-nitrophenol/4-nitrophenol system we also carried out adsorption experiments for fixed initial concentrations (i.e., 3055 and 1455 mg/L for 3- and 4-nitrophenols, respectively) with varying amounts of HDTMA–montmorillonite. Equilibrium concentrations were also determined using the UV-Visible spectrophotometer which correlated absorbances at different wavelengths to the concentrations of the multiple phenolic compounds involved.

FILM-SOLID DIFFUSION MODEL FOR A FINITE BATCH ADSORBER

In order to analyze the adsorption kinetics of the HDTMA cation on the washed montmorillonite, we chose the film-solid diffusion model (11). This model pictures 1) the diffusion of a solute through an external liquid film to the surface of a particle, 2) instantaneous establishment of equilibrium at the surface between the solute on the solid particle and that in the external liquid due to very fast physical adsorption, and 3) subsequent intraparticle diffusion toward center with a constant, effective solid diffusivity, D_s. A schematic for the concentration profile around a particle is depicted in Fig. 1 for visualiza-

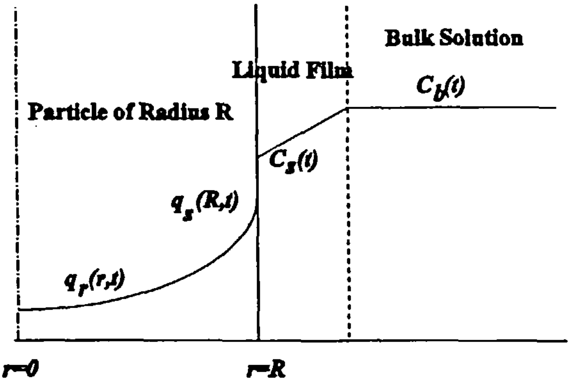

FIG. 1 A schematic for the concentration profile around a particle at time *t*.

tion of the model. Porous particles, usually assumed to be spheres of uniform radius, R, are modeled as a homogeneous solid phase containing no pores.

Mass balance in the spherical solid particle leads to

$$\frac{\partial q_r}{\partial t} = D_s\left(\frac{\partial^2 q_r}{\partial r^2} + \frac{2}{r}\frac{\partial q_r}{\partial r}\right) \tag{1}$$

where q_r represents the solute concentration in the adsorbed phase as functions of both time and radial position, and D_s is the effective solid diffusivity in the particle. Initial and boundary conditions for Eq. (1) are

$$q_r(r, 0) = 0 \tag{2}$$

$$\rho_p D_s \left.\frac{\partial q_r}{\partial r}\right|_{r=R} = k_f(C_b - C_s) \tag{3}$$

$$\left.\frac{\partial q_r}{\partial r}\right|_{r=0} = 0 \tag{4}$$

respectively. In the above equations, C_b denotes solute concentration in the bulk solution phase as a function of time, and k_f, ρ_p, and C_s represent the external liquid film mass transfer coefficient, the pellet density, and the liquid phase concentration at the particle surface, respectively.

For a finite batch adsorber of solution volume V containing adsorbent particles, the mass balance for the solute in the solution becomes

$$V\frac{dC_b}{dt} = -\frac{3k_f W}{\rho_p R}(C_b - C_s) \tag{5}$$

where W denotes the particle mass used in the adsorber. The initial condition for the batch adsorber is

$$C_b(0) = C_0 \tag{6}$$

where C_0 denotes the initial solute concentration in the bulk solution.

Provided an adsorption equilibrium isotherm for a single solute is available to relate $q_r(R, t)$ to $C_s(t)$, these simultaneous equations can be solved numerically to determine C_b against time using the implicit Crank–Nicholson finite difference method (12).

ADSORPTION ISOTHERMS AND COMPETITIVE ADSORPTION MODELS USED

The adsorption isotherms frequently employed for single-component systems are the 2-parameter Langmuir and the 3-parameter Redlich–Peterson

(RP) (13) models. Langmuir and RP models obey the thermodynamic boundary conditions of Henry's law over an infinitely dilute concentration range. The Langmuir and RP models for liquid-phase adsorption are written respectively as follows.

$$q = \frac{q_m bC}{1 + bC} = \frac{aC}{1 + bC} \tag{7}$$

$$q = \frac{\alpha C}{1 + \frac{\alpha}{\kappa} C^{1-(1/\nu)}} \tag{8}$$

where C is the equilibrium solute concentration in the solution phase and q is the equilibrium adsorbed concentration of solute per unit weight of adsorbent. q_m and b in the Langmuir model represent monolayer adsorption capacity and a constant related to adsorption equilibrium constant, respectively, and α, κ, and ν in the RP model are empirical constants.

To analyze multicomponent competitive adsorption behaviors, the Langmuir Competitive Model (LCM) (14–16) and the Ideal Adsorbed Solution Theory (IAST) model (15–18) were used in this study. LCM is an extended form of the Langmuir model which allows predictions of the amount of solute i adsorbed per unit weight of adsorbent, q_i, in the presence of other solutes.

$$q_i = \frac{q_{m,i} b_i C_i}{1 + \sum_{j=1}^{N} b_j C_j} \tag{9}$$

where C_i is the equilibrium concentration of solute i in a mixture consisting of N components, and constants b_i and $q_{m,i}$ are parameters determined by fitting the Langmuir model to the single component adsorption data of solute i alone.

The IAST model, originally proposed by Radke and Prausnitz (18), is of a descriptive nature and requires experimental equilibrium concentrations in the liquid phase to predict the adsorbed solid phase concentrations. To utilize the full predictive power and to simplify the calculation, we followed modifications made by Yen (15, 16), as shown below. IAST is based on the equivalence of spreading pressure in a mixture under equilibrium. The equivalence of spreading pressure in a mixture leads to

$$\int_0^{q_1^\dagger} \frac{d \log C_1}{d \log q_1} dq_1 = \int_0^{q_2^\ddagger} \frac{d \log C_2}{d \log q_2} dq_2 = \cdots = \int_0^{q_N^\S} \frac{d \log C_N}{d \log q_N} dq_N \tag{10}$$

Other equations involved in IAST calculation are

$$C_i = z_i C_i^* \tag{11}$$

$$\sum_{i=1}^{N} z_i = 1 \tag{12}$$

$$q_i^* = f(C_i^*) \tag{13}$$

$$\frac{1}{q_T} = \sum_{i=1}^{N} \frac{z_i}{q_i^*} \tag{14}$$

$$q_i = z_i q_T \tag{15}$$

$$q_i = \frac{V(C_{i,0} - C_i)}{W} \tag{16}$$

In the above equations, C_i and q_i denote equilibrium concentrations in the liquid and adsorbed phases of a solute i in a mixture, respectively z_i is the mole fraction of solute i in the adsorbed phase, and C_i^* and q_i^* refer to equilibrium concentrations in the liquid and solid phases of solute i that adsorbs singly from solution at the same temperature and spreading pressure as those of the mixture, respectively. The function f in $q_i^* = f(C_i^*)$ denotes an adsorption isotherm for solute i. $C_{i,0}$ is the initial concentration of solute i, and q_T is the total adsorbed concentration of all solutes in the mixture. There are $5N + 1$ equations in total, while C_i, q_i, C_i^*, q_i^*, z_i, and q_T comprise a set of $5N + 1$ unknowns. Therefore, we can predict the multicomponent adsorption equilibria, q_i vs C_i, by solving these equations simultaneously.

RESULTS AND DISCUSSION

Kinetic Analysis of HDTMA Adsorption

We applied the film-solid diffusion model to the adsorption kinetics and equilibrium data of HDTMA cation on montmorillonite at 25°C as reported by Kim et al. (4). The adsorption equilibrium isotherm is well described by the Langmuir model:

$$q = \frac{8.61C}{1 + 0.0558C} \tag{17}$$

The adsorption equilibrium data and fitted Langmuir model are shown together in Fig. 2.

Changes in the liquid phase HDTMA concentration, C_b, with time during adsorption are shown in Fig. 3. By fitting the film-solid diffusion model to the experimental kinetic data of Kim et al. (4), the effective solid diffusivity of the HDTMA cation in the washed montmorillonite was estimated to be about 3×10^{-12} cm^2/s. Assuming the effective solid diffusivity of phenolic

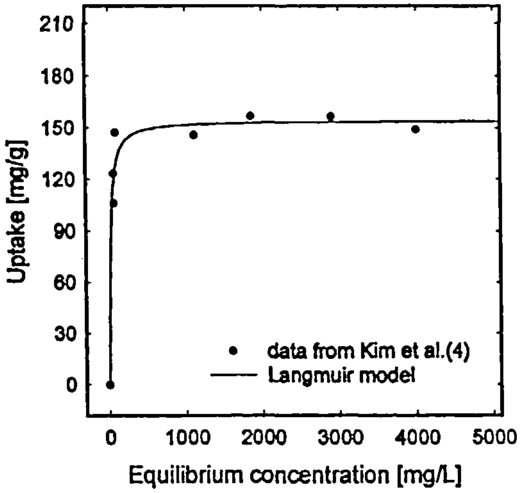

FIG. 2 Adsorption isotherm of HDTMA cation on montmorillonite.

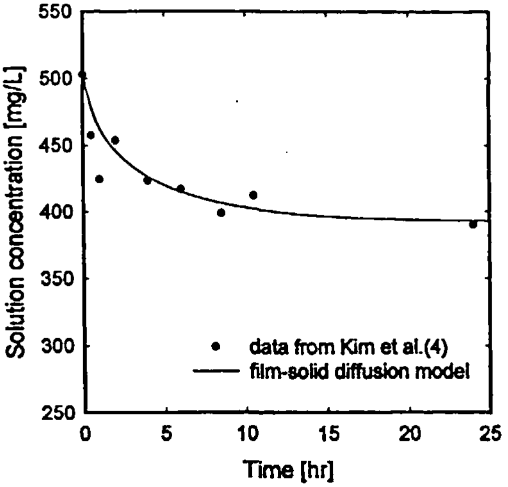

FIG. 3 Adsorption kinetics of HDTMA cation on montmorillonite.

TABLE 2
Physical Parameters Used in the Film-Solid Diffusion Model

Average radius, R	7.5 μm
Pellet density,[a] ρ_p	0.825 g/cm^3
Solution volume, V	0.4 L
Initial concentration, C_0	502.9 mg/L
Mass transfer coefficient, k_f	8×10^{-6} cm/s
Amount of montmorillonite, W	0.3 g

[a] From the characterization sheet provided by the manufacturer.

compounds in activated carbon is around 10^{-8} cm^2/s, an order of 10^{-12} cm^2/s for the HDTMA cation is much lower than expected from the bulkiness of the adsorbate. Computed results from the fitted model are shown together in Fig. 3 for comparison. The physical parameters used in the model are listed in Table 2. The external liquid film mass transfer coefficient was estimated to be 8×10^{-6} cm/s using the initial slope method proposed by Furusawa and Smith (19): since C_s is zero at time zero, combining Eqs. (5) and (6) yields

$$k_f = -\frac{VR\rho_p}{3WC_0}\frac{dC_b}{dt}\bigg|_{t=0} \tag{18}$$

Here, the initial slope, $dC_b/dt|_{t=0}$, was determined from Fig. 3.

Single Component Adsorption of Phenolic Compounds

The single solute adsorption of phenol, 2-, 3-, and 4-nitrophenols was carried out using HDTMA–montmorillonite. Single solute adsorption isotherms on HDTMA–montmorillonite are shown together in Fig. 4 for visual inspection of the adsorption affinity. It is obvious from the figure that nitro-substitution increases the adsorption affinity of phenol on HDTMA–montmorillonite. This point can be explained by the differences in the van der Waals attractive forces between the hydrocarbon tail group of the organic cation and a solute, originating from the differences in molecular weight between phenol and nitrophenol isomers. In the case of adsorption onto activated carbon, however, the adsorptive enhancement of nitrophenols over phenol was explained by the interaction between the carbon surface and the pi electron system of the aromatic ring (20). The carbonyl oxygen on the carbon acts as the electron donor and the aromatic ring of the solute acts as the acceptor. Nitro-substituted phenols thus enhance the donor–acceptor interaction due to the electron-withdrawing nature of the nitro group.

The order of adsorption affinity among the three nitrophenol isomers was found to be 3-nitrophenol ≈ 4-nitrophenol > 2-nitrophenol, clearly exhibiting the effect of the position of substitution between 2-nitrophenol and 3- or 4-nitrophenol, even though isotherm data for 2-nitrophenol is rather limited due to its rather low solubility in water. This is caused by the easy formation of intramolecular hydrogen bonding between an oxygen in the nitro group and a hydroxyl hydrogen. The affinity order agrees with the order of solubility of nitrophenol isomers in water. Suidan (21) reported that the adsorptive ability of either methyl- or chloro-substituted phenol isomers onto activated carbon is dependent upon the position of the functional group. According to Lee et al. (22), the affinity order of nitrophenol isomers on activated carbon is 2-nitrophenol > 4-nitrophenol ≈ 3-nitrophenol, which is roughly in the reverse order of the HDTMA–montmorillonite.

Both the 2-parameter Langmuir and the 3-parameter RP models were fitted to the adsorption data of each phenolic compound by using the nonlinear regression method. Fitted curves of the Langmuir and RP models are shown together in Fig. 4 for comparison, and the parameters of both adsorption models are tabulated in Tables 3 and 4, respectively. The values of the parameter q_m appearing in the Langmuir model again roughly reflect the order of adsorption affinity among nitrophenol isomers. In view of the correlation coefficient values in the tables, both models appear to agree well with the

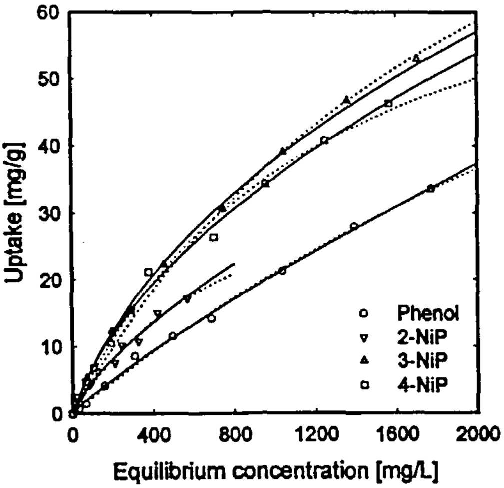

FIG. 4 Single solute adsorption isotherms of phenol and nitrophenol isomers on HDTMA–montmorillonite. Solid and dotted lines represent Redlich–Peterson and Langmuir models, respectively.

TABLE 3
Langmuir Parameters of Each Phenolic Compound on HDTMA–Montmorillonite

Compound	q_m (mg/g)	b (L/mg)	a (L/g)	Correlation coefficient
Phenol	140.1	1.772×10^{-4}	0.02482	0.9972
2-NiP	43.03	11.83×10^{-4}	0.05091	0.9859
3-NiP	128.0	4.225×10^{-4}	0.05407	0.9969
4-NiP	81.52	7.939×10^{-4}	0.06472	0.9938

experimental data considering that the correlation coefficients are greater than 0.99 except for the correlation coefficient of 2-nitrophenol (0.986).

Two-Component Competitive Adsorption of Phenolic Compounds

Two-component competitive adsorptions were performed using the four binary systems phenol/3-NiP, phenol/4-NiP, 2-NiP/3-NiP, and 3-NiP/4-NiP. Single-component adsorption models used in the predictive IAST model were the Langmuir and RP models, the parameters of which were determined from the nonlinear curve fitting the single-component adsorption data mentioned above (see Tables 3 and 4). Both the competitive adsorption data and the predictions of the IAST and LCM models for each binary system are shown in Figs. 5(a) to 5(d). To further clarify the competitive adsorption behavior of two components with similar affinities, like the 3-NiP/4-NiP binary system, we carried out two additional adsorption experiments. One was for the various initial concentrations in a 2:1 concentration ratio with a fixed amount (0.5 g) of HDTMA–montmorillonite and the other for fixed initial concentrations of 3055 mg/L 3-nitrophenol and 1455 mg/L 4-nitrophenol with varying amounts of HDTMA–montmorillonite. Figures 6 and 7 show the experimental results and predictive computations for the former and the latter adsorption schemes, respectively. It is obvious from these figures that the predictive

TABLE 4
Redlich–Peterson Parameters of Each Phenolic Compound on HDTMA–Montmorillonite

Compound	α (L/g)	κ $(\mathrm{mg})^{1-1/\nu} \cdot \mathrm{L}^{1/\nu}/\mathrm{g}$	ν	Correlation coefficient
Phenol	0.05399	0.1815	1.322	0.9979
2-NiP	0.1709	0.3511	1.542	0.9884
3-NiP	0.09961	4.314	2.604	0.9995
4-NiP	0.1260	1.7746	2.082	0.9959

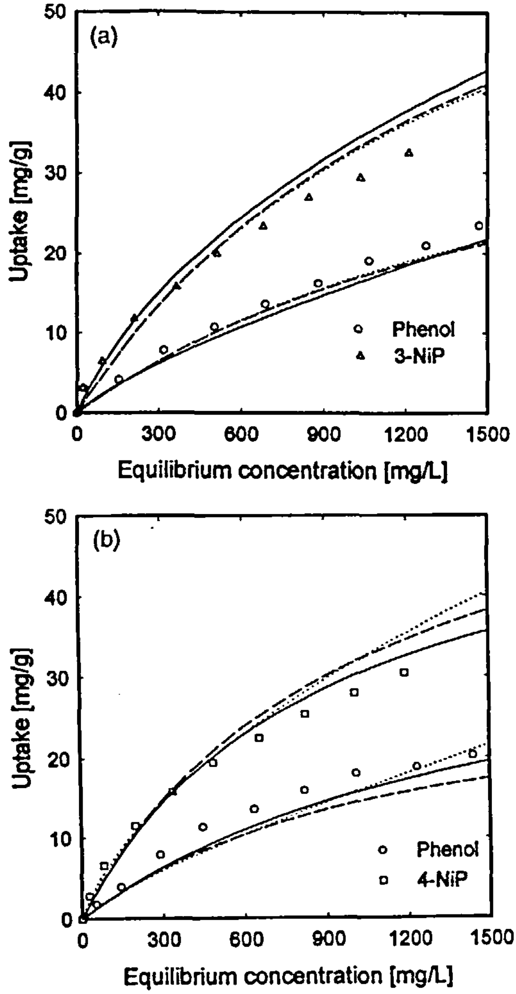

FIG. 5 Adsorption isotherms on HDTMA-montmorillonite of (a) phenol/3-nitrophenol, (b) phenol/4-nitrophenol, (c) 2-nitrophenol/3-nitrophenol, and (d) 3-nitrophenol/4-nitrophenol binary systems with an initial concentration ratio of 1/1. Solid and dotted lines denote IAST predictions based on Redlich–Peterson and Langmuir models, respectively, and dashed lines, LCM predictions.

(continued)

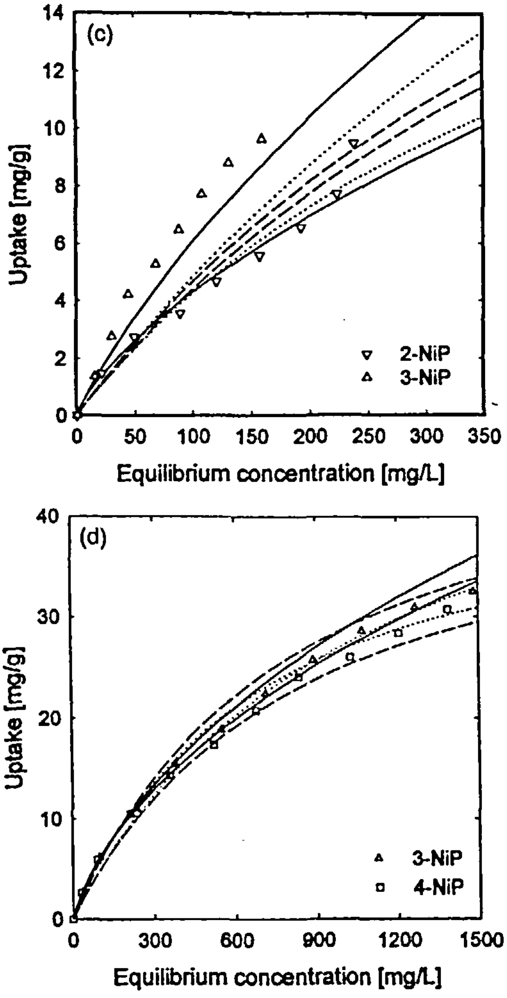

FIG. 5 Continued.

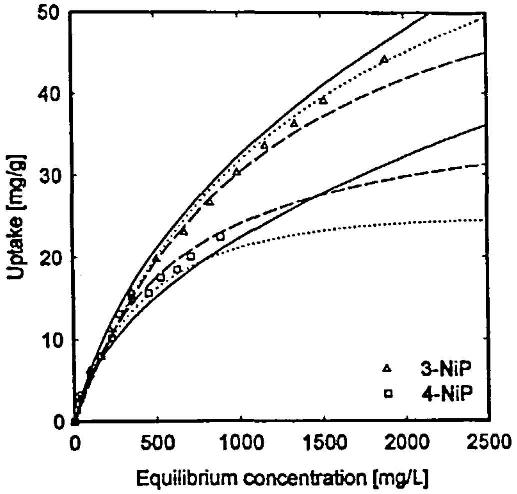

FIG. 6 Adsorption isotherm on HDTMA–montmorillonite of 3-nitrophenol/4-nitrophenol binary system with an initial concentration ratio of 2/1. Solid and dotted lines denote IAST predictions based on Redlich–Peterson and Langmuir models, respectively, and dashed lines, LCM predictions.

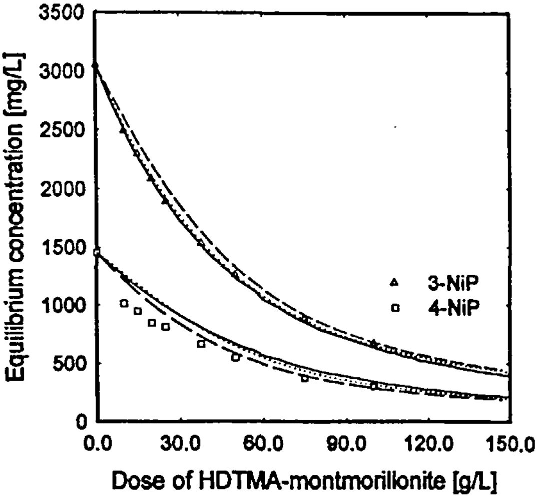

FIG. 7 Adsorption isotherm on HDTMA–montmorillonite of 3-nitrophenol/4-nitrophenol binary system with a fixed initial concentration ratio of 3055/1455. Solid and dotted lines denote IAST predictions based on Redlich–Peterson and Langmuir models, respectively, and dashed lines, LCM predictions.

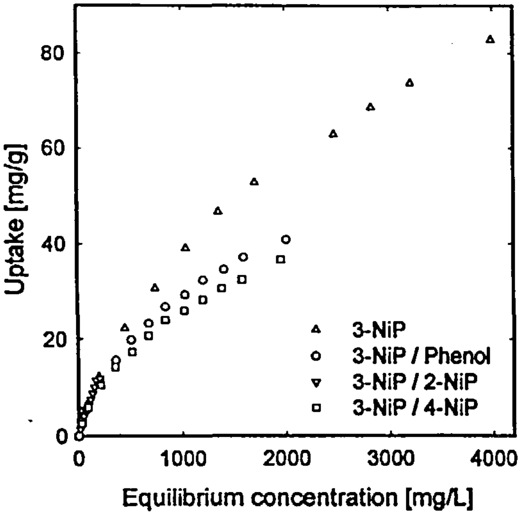

FIG. 8 Single and binary competitive adsorption isotherms of 3-nitrophenol on HDTMA-montmorillonite.

capabilities of both the IAST and LCM models are satisfactory for the binary competitive adsorption of the phenolic compounds on HDTMA–montmorillonite.

One of the main features of adsorption is that the adsorption capacity of a single component is reduced when multiple solutes are present due to the finite adsorption sites available. Figure 8 shows the adsorption isotherms of 3-nitrophenol for the single- and binary-component competitive adsorptions. Adsorption capacities of 3-nitrophenol decrease when other solutes are present due to the competition for the available sites between adsorbable components. This point also establishes the fact that sorption of phenolic compounds onto HDTMA–montmorillonite occurs by an adsorption, not a partition, mechanism.

CONCLUSIONS

The adsorptions of phenol and three nitrophenol isomers on montmorillonite organically modified with HDTMA cation have been studied using single and two adsorbable component systems in aqueous solution at 25°C. By exchanging small cations on the montmorillonite for HDTMA cations, the surface property of montmorillonite has been changed from hydrophilic to organophilic, thus enhancing the sorption capacity for organic contaminants. By fitting the film-solid diffusion model to a set of adsorption kinetic data of HDTMA cation onto the washed montmorillonite, effective solid diffusivity of HDTMA in the montmorillonite was estimated to be about 3×10^{-12} cm^2/s. Both the Langmuir and the RP models were well fitted to single-component adsorption data, while the predictions of the IAST and the LCM models also agreed well with the competitive adsorption data of phenolic compounds on HDTMA–montmorillonite. From the experimental results for both single and competitive adsorption behaviors, it was observed that the adsorption affinity to HDTMA–montmorillonite was in the order 3-nitrophenol ≈ 4-nitrophenol > 2-nitrophenol > phenol. Differences in adsorption affinity among phenol and nitrophenol isomers are possibly due to differences in the van der Waals attractive force caused by differences in molecular weight and the position of substitution of the nitro functional group as well.

ACKNOWLEDGMENT

This paper was supported by Kyungpook National University Research Fund, 1996, for which one of the authors (D.I.S.) expresses his gratitude.

REFERENCES

1. M. M. Mortland, S. Sun, and S. A. Boyd, *Clays Clay Miner.*, *34*, 581 (1986).
2. S. A. Boyd, S. Sun, J. F. Lee, and M. M. Mortland, *Ibid.*, *36*, 125 (1988).
3. S. A. Boyd, M. M. Mortland, and C. T. Chiou, *Soil Sci. Soc. Am. J.*, *52*, 652 (1988).
4. Y. S. Kim, D. I. Song, Y. W. Jeon, and S. J. Choi, *Sep. Sci. Technol.*, *31*, 2815 (1996).
5. J. F. Lee, M. M. Mortland, S. A. Boyd, and C. T. Chiou, *J. Chem. Soc.*, *Faraday Trans. I*, *85*, 2953 (1989).
6. F. Cadena, *J. Environ. Eng.*, *115*, 756 (1989).
7. J. A. Smith and A. Galan, *Environ. Sci. Technol.*, *29*, 685 (1995).
8. J. H. Lee, D. I. Song, and Y. W. Jeon, *Sep. Sci. Technol.*, *32*, 1975 (1997).
9. J. C. Evans and S. E. Pancoski, *Organically Modified Clays*, Preprints, Paper 880587, Transportation Research Board, 68th Annual Meeting, January 22–26, 1989, Washington, DC.
10. H. van Olphen, "Note on the Preparation of Clay Suspension," in *Clay Colloid Chemistry*, 2nd ed., Wiley, New York, NY, 1977.
11. K. E. Noll, V. Gounaris, and W.-S. Hou, *Adsorption Technology for Air and Water Pollution Control*, Lewis Publishers, Chelsea, 1992.
12. J. B. Riggs, *An Introduction to Numerical Methods for Chemical Engineers*, 2nd ed., Texas Tech University Press, Lubbock, TX, 1994.
13. O. Redlich and D. L. Peterson, *J. Phys. Chem.*, *63*, 1024 (1959).
14. J. A. V. Butler and C. J. Ockrent, *Ibid.*, *34*, 2841 (1930).
15. C. Y. Yen, "The Adsorption of Phenol and Substituted Phenols on Activated Carbon in Single- and Multi-Component Systems," Ph.D. Dissertation, University of the North Carolina at Chapel Hill, 1983.
16. C. Y. Yen and P. C. Singer, *J. Environ. Eng.*, *110*, 976 (1984).
17. Y. W. Jeon and C. W. Curtis, *Fuel Sci. Technol. Int.*, *10*, 697 (1992).

18. C. J. Radke and J. M. Prausnitz, *AIChE J.*, *18*, 761 (1972).
19. T. Furusawa and J. M. Smith, *Ind. Eng. Chem. Fundam.*, *12*, 197 (1973).
20. J. S. Mattson and H. B. Mark, *Activated Carbon-Surface Chemistry and Adsorption from Solution*, Dekker, New York, NY, 1971.
21. M. T. Suidan, *Oxidative Coupling of Phenols on Activated Carbon Impact on Adsorption Equilibria*, Presented at the Korea–America Environment Symposium on Clean Water Treatment Technology, Seoul, South Korea, 1995.
22. B. S. Lee, K. S. Ha, and J. B. Kim, *J. Korean Inst. Chem. Eng.*, *26*, 583 (1988).

Received by editor September 17, 1997
Revision received February 1998